Structural Characterization of POPC and $C_{12}E_4$ in Their Mixed Membranes at Reduced Hydration by Solid State ^2H NMR

Gotthard Klose,*,† Burkhard Mädler,† Hartmut Schäfer,‡ and Klaus-Peter Schneider†

Fakultät für Physik und Geowissenschaften, Institüt für Experimentelle Physik I, Universität Leipzig, BIM, Linnéstrasse 5, D-04103 Leipzig, Germany, and HF-NMR Facility, NSR Center, University of Nijmegen, Toernooiveld 1, 6525 ED Nijmegen, The Netherlands

Received: August 26, 1998; In Final Form: January 13, 1999

Structural characteristics of the palmitoyl and dodecyl chains as well as of the headgroups of POPC and $C_{12}E_4$, respectively, were determined at 25 °C in the pure and mixed (surfactant lipid molar ratios $R_{S/L} = 0.2$ and 1) membranes hydrated at the same relative humidity of 97% by deuterium NMR using partially deuterated lipids (POPC-d_{31} and POPC-d_4) and surfactants ($C_{12}E_4$-d_{25} and $C_{12}E_4$-d_{16}). At $R_{S/L} = 0.2$ the surfactant causes a rigidization of the membrane evidenced by the reduction of the cross-sections of the hydrocarbon chains, mainly of that of the surfactant dodecyl chain, whereas at $R_{S/L} = 1$ fluidization of the membrane occurs due to the mismatch of the hydrocarbon chain lengths. The surfactant dodecyl chain penetrates the membrane to the same depth as the first twelve methylene segments of the lipid palmitoyl chain. Experiment and Monte Carlo simulation show that the mean orientation of the lipid headgroup simultaneously changes toward the membrane director whereas the headgroup structure adopts a pearlike shape within the lipid matrix ($R_{S/L} = 0.2$), which changes its shape, increasing the surfactant concentration ($R_{S/L} = 1$). Conclusions on the prevailing interactions have been drawn. The successful analysis of the surfactant headgroup ^2H NMR spectra adds a new example to the potentialities of the modified de-Pakeing techniques developed by Schäfer et al.[22,23]

1. Introduction

Lipid/nonionic surfactant mixtures have great potentialities not only as a useful tool in membrane biochemistry as they are suitable for membrane solubilization,[1,2] disruption of bilayers, protein extraction[3,4] and reconstitution[5] but also as model systems for studying fundamental questions,[6−10] for instance the interrelation of hydration,[11] structural,[12] and dynamic properties[13] in complex systems.

The ternary phase behavior of POPC/$C_{12}E_4$/water mixtures in the whole concentration range of their components was determined.[6] It was found that at 25 °C the liquid-crystalline lamellar phase (L_α) occupies the largest area in the triangle phase diagram. That means in the frame of Israelachvili's packing concept[14] that the compound molecules formed of POPC and $C_{12}E_4$ possess cylinder-like effective shapes in large ranges of composition. This can only be realized if the lipid and surfactant molecules are correspondingly arranged in the mixed membranes. First, direct information about the location of the surfactant in the lipid matrix was obtained by applying X-ray and neutron diffraction.[12] According to this study, the first (α-) methylene segment of the surfactant dodecyl chain is anchored just at the boundary of the hydrophobic core of the mixed membranes. Sorption measurements in combination with X-ray diffraction as a function of both the composition and the length of the surfactant ethylene oxide chain yielded more structural details.[11] It was found that at small $C_{12}E_4$ concentrations the thicknesses of the bilayer and of the hydrophobic core are bigger compared to pure POPC membranes and that they both progressively decrease with increasing surfactant concentration. These quantities characterize the mixed membranes only, but they do not allow us to derive values for the single contributions resulting from the individual components. Further (see ref 11), we determined the surface requirements of the components and found that at low surfactant concentrations the area requirement of the lipid is smaller and that of the surfactant is bigger compared with the corresponding pure membranes under the same conditions (temperature, hydration pressure). Though the procedure applied for gaining the quantitative values seemed to be reliable, the conclusions drawn need to be ensured.

The main aim of this work is to determine detailed structural characteristics of the hydrocarbon chains as well as the headgroups of the individual components, POPC and $C_{12}E_4$, in the mixed membrane, which allows us to understand or to prove the results obtained by the scattering studies[11,12] on one hand and to come to an agreement on the determining interactions between the lipid and surfactant molecules on the other hand.

For this purpose ^2H NMR was applied. It provides a very convenient way to determine the order of molecules in liquid crystalline phases and allows us to describe the spectral parameters in terms of the molecular structure (see, e.g., refs 15−17).

In the study presented here we used partially alkyl chain and headgroup-deuterated lipids (POPC-d_{31} and POPC-d_4) and surfactants ($C_{12}E_4$-d_{25} and $C_{12}E_4d_{16}$) in order to be able to determine the individual structural characteristics of each component in the mixed membranes.

The results obtained by NMR in this work together with X-ray diffraction and sorption isotherm data published in refs 11 and 12 yield a detailed structural picture that enables qualitative conclusions about the determining interactions. In particular, Monte Carlo simulations allow for the conclusion that the

* Corresponding author. E-mail: klose@physik.uni-leipzig.de. Fax: +341 97 32 479.
† Universität Leipzig.
‡ University of Nijmegen.

10.1021/jp983528n CCC: $18.00
Published on Web 03/30/1999

orientation of the lipid headgroup is clearly influenced by electrostatic interactions. Besides this the results confirm conclusions drawn in ref 11.

2. Materials and Methods

Substances and Sample Preparation. The partially deuterated phospholipids 1-palmitoyl-2-oleoyl-sn-glycero-3-phosphocholines POPC-d_{31} (deuterated palmitoyl chain) and POPC-d_4 (deuterated methylene groups of the choline group) were purchased from Avanti Polar Lipids/USA and used without further purification. The POPC-d_{31} and POPC-d_4 contain impurities of some weight percent evidenced by the presence of additional lines in the de-Paked ^{2}H NMR spectra (cf. Figures 1 and 3). This is probably due to 1-oleoyl-2-palmitoyl-sn-glycero-3-phosphatidylcholine (OPPC), which is formed by transmigration of the chains. Morrison and Bloom[18] also detected such contamination in POPC-d_{31} originating from Avanti Polar Lipids. However, the presence of OPPC to some percents does not influence our results.

The partially deuterated tetra(ethylene oxide) monododecyl ethers $C_{12}E_4$-d_{25} (deuterated dodecyl chain) and $C_{12}E_4$-d_{16} (deuterated methylene groups of the ethylene oxide chain) were chemically synthesized as described in ref 12.

Lipid surfactant mixtures with the surfactant to lipid molar ratios $R_{S/L} = 0.2$ and 1.0 were prepared in the following way: Approximately 20 mg of lipid was mixed with the appropriate amount of surfactant and dissolved in ethanol. The solvent was evaporated under a stream of nitrogen and further under vacuum conditions (10^{-3} Pa) for 10 h. The samples including those of the pure compounds were hydrated with deuterium-*d*epleted water vapor at a relative humidity RH = 97% and at 25 °C inside an airtight sorption balance, giving the hydration pressure of 4.19 MPa. It correlates with water concentrations of 13.0 (pure POPC), 7.5 (pure $C_{12}E_4$), 9.5 ($R_{S/L} = 0.2$), and 19.0 ($R_{S/L} = 1$) molecules of water per molecule of amphiphile (lipid plus surfactant) with an error of ±0.5 water molecules. Details are described in ref 19.

^{2}H NMR. The ^{2}H NMR spectra were recorded at 76.7 MHz on a Bruker MSL 500 spectrometer at 25 °C. Between 2048 and 16 384 scans, depending on the amount of the deuterated nuclei in the mixture, were necessary for a sufficiently good signal-to-noise ratio. To avoid phase errors a quadrupolar echo sequence $(\pi/2)_y - t_1 - (\pi/2)_x - t_2 -$FID ($\pi/2 = 2.7$ μs, $t_1 = 40$ μs) with quadrature phase cycling and a repetition time of 750 ms were applied. t_2 was carefully chosen to start the accumulation of the FID at the echo top. The quadrature channels were adjusted for minimal signal intensity in the imaginary time domain channel to achieve a satisfying symmetric quadrupole powder spectrum. The Fourier transformation was applied without any line broadening and phase correction.

Data Analysis. *NMR.* In the case of axially symmetric molecular motion like in lamellar liquid crystalline phases, where the bilayer normal is an axis of motional averaging ^{2}H NMR of a planar bilayer, the *i*th C−D alkyl segment yields two symmetric resonance lines, the distance between which is defined as quadrupolar splitting according to

$$\Delta\nu_q^{(i)} = \frac{3}{2}\hat{Q}P_2(\cos\theta)\, S_{CD}^{(i)} \tag{1}$$

with the static quadrupolar coupling constant $\hat{Q}$ 170 kHz for a C−D bond (see, e.g., ref 15) $P_2 = {}^1/_2(3\cos^2\theta - 1)$ is the second-rank Legendre polynomial and θ is the angle between the bilayer normal and the static magnetic field. The C−D bond order can be expressed by the CD-bond order parameter

$$S_{CD}^{(i)} \equiv \langle P_2(\cos\varphi_i)\rangle = \frac{1}{2}\langle 3\cos^2\varphi_i - 1\rangle \tag{2}$$

as a time-averaged value for the angle fluctuations φ_i between the C−D bond of the *i*th segment in the alkyl chain and the bilayer normal (the reduced axis of molecular motion).

The measured ^{2}H NMR powder spectra are a result of an integration over all orientations θ of the director (bilayer normal) with respect to the static magnetic field with the appropriate probability $P(\theta)\ \mathrm{d}\theta = \sin\theta\ \mathrm{d}\theta$ for a liposomal dispersion (powder distribution). This typical spectrum pattern is called *Pake-Dublett* or *Pake-Powder spectrum* (see, e.g. ref 15).

The distance between the intense central lines is denoted as the quadrupolar splitting of the *i*th C−D bond corresponding to $\theta = 90°$. Therefore eq 1 results into

$$\Delta\nu_q^{(i)} = \frac{3}{4}\hat{Q}S_{CD}^{(i)} \tag{3}$$

The common *de-Pakeing* procedure deconvolutes the experimental spectra to subspectra corresponding to the $\theta = 0°$ orientation. An order parameter profile can be directly obtained from the de-Paked spectra, only assuming a monotonic decrease of $S_{CD}^{(i)}$ along the alkyl chain from the polar−apolar interface of the bilayer to the terminal methyl group in the middle of the hydrophobic membrane core.[20] In this approach we used a new de-Pakeing procedure by means of *Tikhonov Regularization*,[21] which has already been substantially tested in different manners,[22,23] mainly with simulation character. In this study we present the advantages and significant improvements of the new method especially under conditions of low signal-to-noise ratios and/or strong individual line broadening in relation to the overall splitting of the NMR powder spectra (cf. Figure 4).

The ^{2}H NMR spectrum of an oriented sample $S_0(\omega)$ can be calculated from the spectrum of the corresponding powder sample $S(\omega)$ solving a Fredholm-integral equation of the first kind:[21]

$$S(\omega) = \int_{-\infty}^{+\infty} S_0(\omega_0)\, C(\omega_0, \omega)\, \mathrm{d}\omega_0 \tag{4}$$

where the integral kernel $C(\omega_0, \omega)$ is defined as

$$C(\omega_0, \omega) = [3\omega_0(2\omega + \omega_0)]^{-1/2} \tag{5}$$

in the range $-1/2 < \omega/\omega_0$ and $C(\omega_0, \omega) = 0$ else.

The Tikhonov regularization with the self-consistency method and the nonnegative restriction ($S_0(\omega_0) \geq 0$) by Schäfer et al.[22] provides much better approximation for $S_0(\omega_0)$ in eq 4 than the conventional De-Pakeing, especially at poor signal-to-noise ratios occurring in samples that contain only small concentrations of the deuterated component.

Now eq 4 is solved by minimizing

$$\Psi(\lambda) = \sum_{j=1}^{m}\frac{1}{\sigma_j}\left(\zeta_j^{\sigma} - \int_{-\infty}^{+\infty} S_0(\omega_0)\, C(\omega_0, \omega_j)\, \mathrm{d}\omega_0\right)^2 + \lambda\left|\left|\frac{\partial^2}{\partial\omega_0^2}S_0(\omega_0)\right|\right|_{L_2}^2 \tag{6}$$

where a reliable value of the regularization parameter λ is well-defined by the self-consistency method. The m data points ζ_j^{σ} consist of an exactly defined term $S(\omega_j)$ and a noise value ϵ_j

$$V_j^S = S(\omega_j) + \epsilon_j \qquad j = 1, ..., m \tag{7}$$

Even adaptation of that algorithm can be used for the analysis of inversion recovery experiments in the case of anisotropic T_1 relaxation[24] and for nonisotropic orientational distributions, for example orientations or deformations of spherical liposomes due to strong magnetic fields.[23]

The order parameters $S_{CD}^{(i)}$ deduced from the De-Paked spectrum were finally used for the estimation of structural properties of the molecules in the bilayer.

The average projection of the palmitoyl chain length of the lipid $\langle l^L_h \rangle$ and that of the dodecyl chain of the surfactant $\langle l^S_h \rangle$ along the all-trans state, which is aligned with the bilayer normal, were calculated by applying a simple statistical model.[25,26] It yields a value for the hydrophobic bilayer thickness $d_h = 2\langle l_h \rangle$ where

$$\langle l_n \rangle = l_0/2[(n-1) + \sum_i^n S_{mol}^{(i)}] \tag{8}$$

with $l_0 = 0.125$ nm, the projection of the C−C bond length onto the hydrocarbon chain axis, and n the number of methylene and methyl groups in the hydrocarbon chain. $S_{mol}^i = |-2S_{CD}^i|$ and $S_{mol}^i = |-6S_{CD}^i|$ are the segmental order parameters for methylene and methyl groups,[27] respectively.

Finally, its cross-section

$$A_h = V_h/\langle l_h \rangle \tag{9}$$

was estimated from the length of the hydrocarbon chain. V_h is the volume of the hydrocarbon chain calculated as sum of the segmental volumes using 0.028 nm^3 for the methylene and 0.056 nm^3 for the methyl groups.[28]

Monte Carlo Simulation. The ^{2}H NMR data of the lipid headgroup were interpreted on the basis of Monte Carlo simulations. In a crude approximation the lipid headgroups were considered as hard disks carrying electric dipoles. A hard disk can move in the membrane plane (x, y plane) and the angle β between the dipole axis and the plane, as well as the orientation of the dipole projection on the plane can change. The presence of nonionic surfactant was taken into account by means of polarizable gaps between the disks, which means corresponding disks were replaced by free areas. In the frame of this simple model the incorporation of surfactant molecules into the lipid matrix is regarded only as a dilution of the lipid molecules. The pair interaction potential of two lipid headgroups i and j includes contributions from hard disk and electric dipole interactions:

$$V_{ij} = V_{ij}^{disk} + V_{ij}^{dipole} \tag{10}$$

where

$$V_{ij}^{disk} = \begin{cases} 0 & \text{for } r_{ij} \geq \sigma \\ \infty & \text{for } r_{ij} < \sigma \end{cases} \tag{11}$$

and

$$V_{ij}^{dipole} = \frac{q^2}{4\pi\epsilon_0\epsilon_r}\left(\frac{1}{|\vec{r}_{i+} - \vec{r}_{j+}|} + \frac{1}{|\vec{r}_{i-} - \vec{r}_{j-}|} - \frac{1}{|\vec{r}_{i-} - \vec{r}_{j+}|} - \frac{1}{|\vec{r}_{i+} - \vec{r}_{j-}|}\right) \tag{12}$$

σ is the diameter of the disks and q is the dipole charge. ϵ_0 and ϵ_r are the electric permittivity (dielectric constants) of the vacuum and of the medium, respectively. $\vec{r}_+$ and $\vec{r}_-$ are the position vectors of the positive and negative dipole charges, respectively, symmetrically arranged with respect to the disk plane.

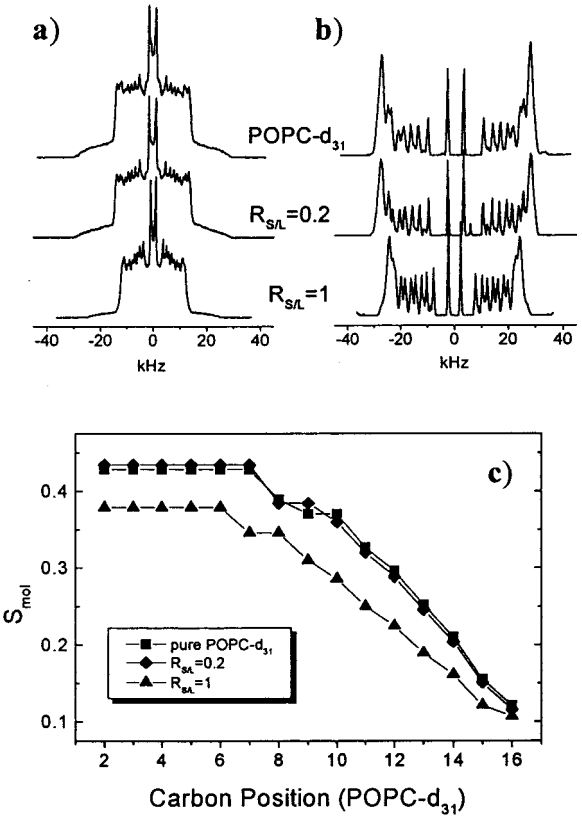

Figure 1. ^{2}H NMR powder (a) and de-Pake-ed ($\Theta = 0°$) spectra (b) of the palmitoyl chain of pure POPC-d_{31} and with $C_{12}E_4$ mixed ($R_{S/L} = 0.2$ and 1) membranes at 25 °C and segmental order profiles (c). The order parameters are connected by lines for clarity.

In the calculations, which are performed using the standard Metropolis algorithm, 400 particles were considered with periodic boundary conditions. The following parameters were assumed: Dipole charge $q = 0.8$ elementary charges, disk diameter $\sigma = 6.8$ Å, dipole length 4 Å, relative electric permittivity (dielectric constant) $\epsilon_r = 20$. The cutoff has been set according to the minimum image convention. This has been proved to be a successful criterion in order to draw semiquantitative conclusions. A detailed description of the model and error sources as well as preliminary results can be found in ref 29.

3. Results

Figures 1 and 2 show the ^{2}H NMR powder and de-Pake-ed spectra together with the segmental order parameter profiles of the palmitoyl chain of the lipid and of the dodecyl chain of the surfactant in the pure and mixed ($R_{S/L} = 0.2$ and 1.0) membranes, respectively. Under our experimental conditions, the deuterium splittings of the first methylene segments of the lipid palmitoyl chain could not be resolved (cf. de-Pake-ed spectra, Figure 1b). Therefore, we assigned the same splitting value to them, corresponding to the difference of the maxima of the intensive outer lines, though it is known that these methylene groups exhibit slightly different splittings.[30] In the de-Pake-ed spectra, some lines of low intensity are present, which results from contamination probably mainly with OPPC (see also substances and sample preparation).

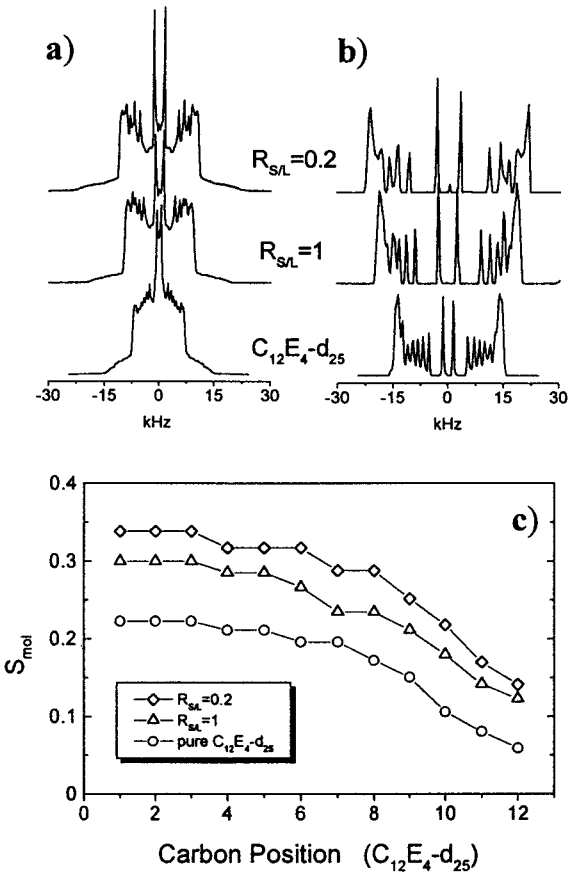

Figure 2. ^{2}H NMR powder **(a)** and de-Pake-ed ($\Theta = 0°$) spectra **(b)** of the dodecyl chain of pure $C_{12}E_4$-d_{25} and with POPC mixed ($R_{S/L}$ = 0.2 and 1) membranes at 25 °C and segmental order profiles **(c).** The order parameters are connected by lines for clarity.

The order parameter profiles of the lipid palmitoyl chain of all samples exhibit similar patterns, namely a relatively broad plateau for the first 5 to 6 methylene groups followed by a considerable reduction of the order parameters of the C_8 and C_9 segments ($R_{S/L} = 0$ and 0.2) or the C_7 segment ($R_{S/L} = 1$) and then a monotonic decrease approaching the terminal methyl group (cf. Figure 1c).

The deuterium splittings of the surfactant dodecyl chain could be quite well resolved for all excepting the first three methylene segments. Next to the plateau formed by the order parameters of the first three methylene segments, the order parameter decreases along the chain approaching the terminal methyl group (Figure 2c). But there are subtle deviations. In the mixed membranes ($R_{S/L} = 0.2$ and 1) the order parameters of the C_7 and C_8 segments differ only slightly in contrast to those in the pure surfactant membrane. This fact can be more clearly deduced from the de-Pake-ed spectra (Figure 2b). While the corresponding lines in the pure surfactant L_α phase appear separately, they almost superimpose in the mixed membranes.

The order parameters of the dodecyl chain in the pure surfactant membrane are smaller by about the factor of 0.5 compared with the corresponding parameters of the palmitoyl chain in the pure lipid membrane under the same conditions.

The incorporation of a small amount of surfactant ($R_{S/L} = 0.2$) into the lipid matrix shifts the order parameter profile of the dodecyl chain about 0.11 to higher values while the ordering of the lipid palmitoyl chain remains almost unaffected (compare Figures 1c and 2c). The increase of the surfactant concentration ($R_{S/L} = 1$) decreases the ordering of the surfactant dodecyl chain as well as that of the lipid palmitoyl chain.

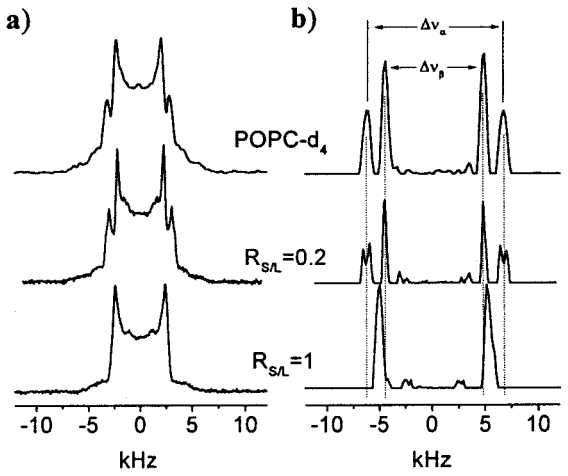

Figure 3. ^{2}H NMR powder (a) and de-Pake-ed ($\Theta = 0°$) spectra (b) of the choline methylene segments of pure POPC-d_4 and with $C_{12}E_4$ mixed ($R_{S/L}$ = 0.2 and 1) membranes at 25 °C.

Figure 3 shows the ^{2}H NMR powder and the de-Pake-ed spectra of POPC-d_4. The signals of low intensity in the central part of the spectra may be probably caused by a contamination with OPPC (see also Substances and Sample Preparation).

Addition of surfactant decreases the quadrupole splitting of the α- and increases that of the β-methylene groups but to a much lower extent. At $R_{S/L} = 1$ they superimpose. It is interesting that at $R_{S/L} = 0.2$ the CD bonds of the α-methylene group become nonequivalent, which is visible from the splitting of the outer lines (cf. Figure 3).

The ^{2}H NMR powder and de-Pake-ed spectra of $C_{12}E_4$-d_{16} and the profiles of the absolute values of the quadrupolar splitting are drawn in Figure 4. The de-Pake-ed spectra (Figure 4b) impressively exhibit the preference of the new de-Pakeing method compared with the conventional one. Only in consideration of an orientation-independent Gaussian line broadening of 110 Hz for the powder spectra, as described in ref 22, was it possible to resolve all methylene splittings of the ethylene oxide chain with their appropriate integrals.

The assignment of the splittings to the methylene groups along the ethylene oxide chain corresponding to their decreasing absolute values is very likely since every single bond increases the degree of motional freedom. It is surprising that the splitting of the first methylene segment of the surfactant does absolutely not change, if the surfactant is incorporated into the lipid matrix ($\Delta\nu = 10.5$ kHz for $R_{S/L} = +\infty$, 0.2 and 1).

In Figure 5 the results of the MC simulations are represented. The pictures above show snapshots of the distribution of the dipole projection on the membrane surface (x, y plane). A tendency of partial separation of lipid and surfactant molecules is visible at $R_{S/L} = 1$ and 2. The probability density $\rho(\beta)$ of the angle β between the electric dipole moment, which can be supposed to be in parallel with the phosphorus nitrogen connecting vector of the lipid headgroup and the membrane plane drawn below, is shifted to larger angles with increasing surfactant concentration in the membrane. In the pure lipid membrane, the headgroup is preferentially oriented in parallel to the membrane, which agrees with experimental findings and other calculations.[31−34]

4. Discussion

We will qualitatively discuss the results obtained in the mixed membranes with respect to the pure lipid and surfactant membranes. Correspondingly, the estimated geometrical pa-

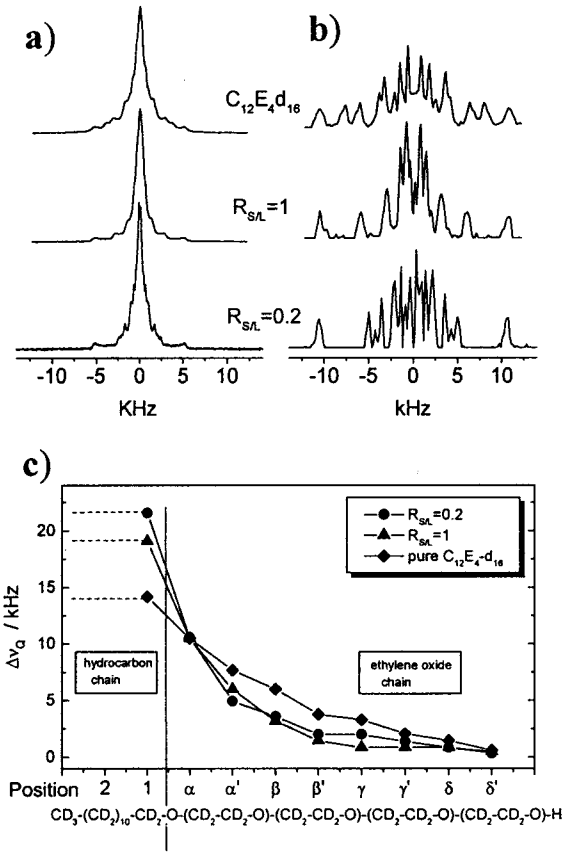

Figure 4. ^{2}H NMR powder (a) and de-Pake-ed ($\Theta = 0°$) spectra (b) of the ethylene oxide chain of pure $C_{12}E_4$-d_{16} and with POPC mixed ($R_{S/L} = 0.2$ and 1) membranes at 25 °C and splitting profiles (c). The ^{2}H splittings are connected by lines for clarity.

rameters, length, and cross-section of the hydrocarbon chains of the components are also used only as relative measures of the quantitatives.

Pure Membranes. At first we will start considering some properties of pure POPC and $C_{12}E_4$ membranes that are important for the discussion of their mixtures. As is known, the acyl chains of the POPC molecules in the membrane are less ordered compared with those of saturated lipids such as, e.g., DMPC or DPPC in the liquid crystalline lamellar state. This is due to steric interactions (constraints) caused by the C—C═C—C fragment of the oleoyl (sn-2) chain in cis conformation. The relatively small order parameters (absolute values) for the C_9 and C_{10} segments measured[30] can be explained mainly by the orientations of the C—D bonds.[35,36] The relatively large and rigid cis-fragment of the unsaturated acyl chain and its orientation lead to disturbances in the saturated palmitoyl chain that result in more motional freedom of neighboring methylene groups, in other words, the cis-fragment creates more free volume, which should be indicated by reduced order parameters. Indeed, our experiments show this effect for the C_8 and C_9 methylene segments of the palmitoyl chain (cf. Figure 1c; order parameter profile for $R_{S/L} = 0$). The same was found also by Seelig and Waespe-Sarcevic,[30] but it was not discussed. The drop of order parameters is reproduced also by the MD results of Heller.[35]

The packing of the dodecyl chain in the pure surfactant membrane is determined by the balance of the hydrophobic and van der Waals attractions on one hand and steric repulsion of the ethylene oxide chains on the other hand. These repulsions result from a larger area requirement of the ethylene oxide chain due to its conformation and hydration compared with the cross-section of the hydrocarbon chain. The repulsions are the main reason, besides the shorter hydrocarbon chain length, that the surfactant hydrocarbon chains in the pure surfactant membrane are less ordered compared with the acyl chains in the pure lipid membrane under the same conditions. One can visualize the different ordering of the lipid and surfactant hydrocarbon chains by considering the order parameters of one component with respect to those of the other one. The differences of the segmental order parameters of the first 12 lipid methylene segments of POPC and those of the corresponding hydrocarbon segments of the surfactant are drawn in Figure 6a. As the drawing for $R_{S/L} = 0$ demonstrates, all the surfactant chain order parameters are 0.21 ± 0.4 smaller than those of the corresponding segments of the lipid palmitoyl chain.

The order parameters of the surfactant dodecyl chain decrease continuously from the C_3 methylene segment, approaching the terminal methyl group (cf. Figure 2c). Though we could not unambiguously resolve the splittings of the first three dodecyl methylene segments, it is likely that the membrane is most tightly packed (largest order parameter) around the C_3 methylene segment as found in membranes of totally deuterated $C_{12}E_4$ in excess water.[37]

The constancy of $S^{(i)}_{mol}(POPC) - S^{(i)}_{mol}(C_{12}E_4)$ implies that the courses of the lipid and the surfactant order parameter profiles of the first 12 hydrocarbon segments are the same. This is surprising since the determining interactions for the ordering in the pure membranes are very different. Maybe this coincidence of the order parameter profiles is accidental or, more likely, it is the result of the same hydration pressures applied.

Mixed Membranes, Hydrocarbon Chains. Incorporation of a small amount of surfactant ($R_{S/L} = 0.2$) into the POPC matrix significantly increases the ordering of the surfactant dodecyl chain (compare Figure 2c, order parameter profiles for $R_{S/L} = 0.2$ and 0). The increase of the ordering correlates with the increase of the hydrocarbon chain length (eq 8) and the reduction of its cross-section (Table 1).

The stretching of the surfactant hydrocarbon chain is mainly the result of the reduction of ethylene oxide repulsions caused by the relatively large mean distance between the surfactant molecules in the membrane. In this respect the lipid molecules act as lateral spacers between the surfactant molecules. But also the interaction of dodecyl chains with the better ordered lipid acyl chains contributes somehow.

In contrast to the ordering of the surfactant dodecyl chain the ordering of the lipid palmitoyl chain is almost not influenced by incorporating small amounts of surfactant (compare Figure 1c, order parameter profiles for $R_{S/L} = 0.2$ and 1.0). The small differences of the order parameter values of pure POPC and of the mixed POPC/surfactant membranes ($R_{S/L} = 0.2$) correspond with the negligible chain length variation (cf. first row of Table 1). The low effect of small amounts of surfactant on the ordering of the lipid palmitoyl chain is expected, since at $R_{S/L} = 0.2$ only one surfactant hydrocarbon chain per 10 lipid acyl chains is present in the mixture. But there is an indirect indication that the surfactant must have certain effects on the lipid palmitoyl chain despite its low concentration. Namely, in the case of saturated lipids, as in DMPC and DPPC in the liquid crystalline lamellar state, the length of the palmitoyl chain decreases already by incorporating low surfactant amounts[8,38] whereas it remains almost unaffected in the case of POPC.

It is likely that the surfactant has a greater effect on the lipid oleoyl chain because the drastically reduced area requirement found for the lipid in the mixed membranes (see Introduction) must mainly result from changes in the oleoyl chain, if the

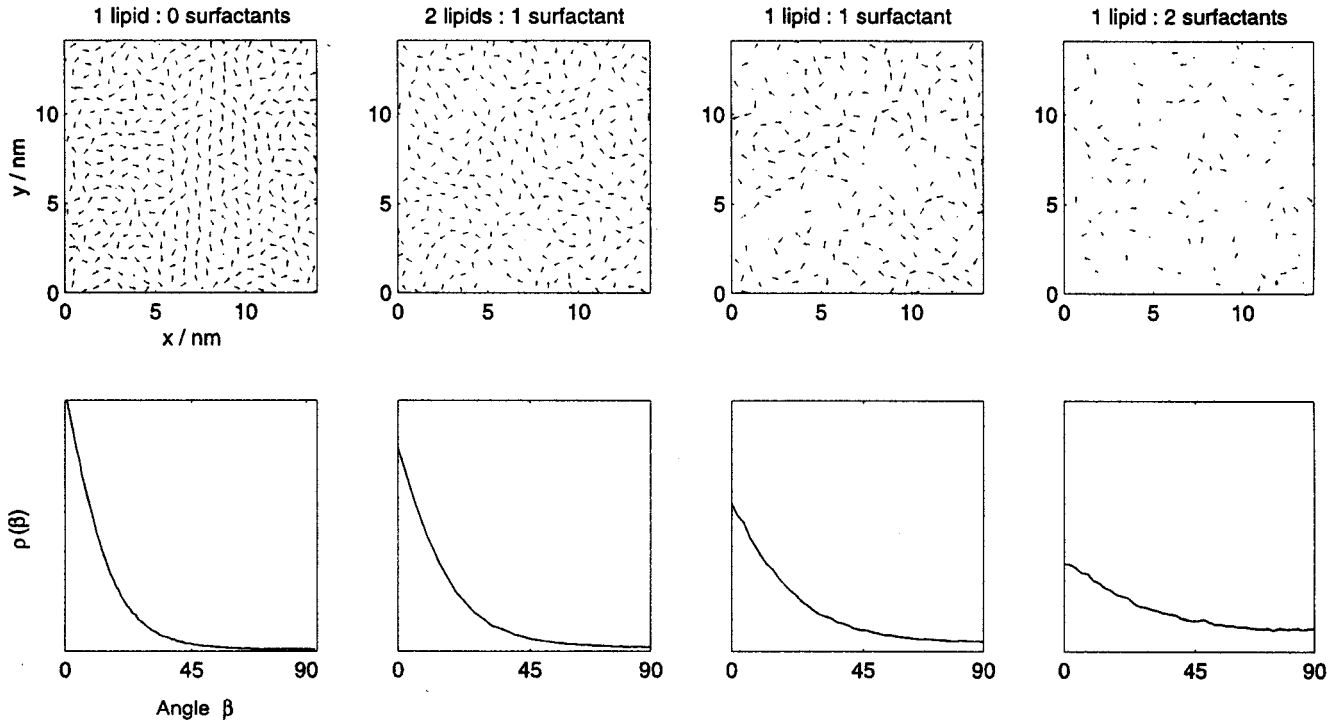

Figure 5. Snapshots of the projection of the lipid headgroup electric dipole moment onto the membrane (x, y) plane (above) and the probability density $\rho(\beta)$ of the angle β between the dipole moment and the membrane plane (below) for $R_{S/L} = 0.3$, 1, and 3 according to MC simulations (see text).

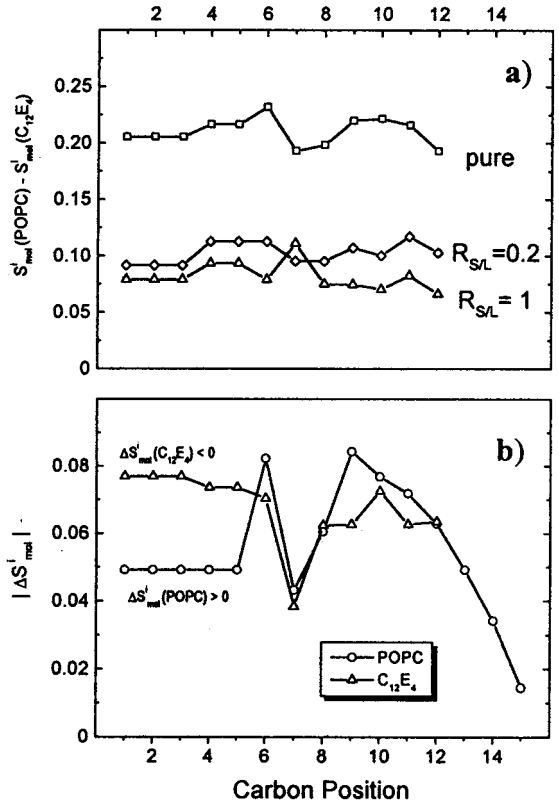

Figure 6. Difference of the order parameters of the corresponding lipid and surfactant segments, $S^i_{mol}(POPC) - S^i_{mol}(C_{12}E_4)$ (a) and the order parameter difference profiles $\Delta S^i_{mol} = S^i_{mol}(\text{pure membrane}) - S^i_{mol}(\text{mixed membrane})$ for the lipid palmitoyl (Δ) and the surfactant dodecyl (○) chains (b) at $R_{S/L} = 1$. The numbering begins with the first methylene segment. The symbols are connected by lines for clarity.

ordering of the palmitoyl chains has hardly changed. Probably, in the presence of the surfactant, the lipid oleoyl chains are able to adopt conformations that yield a tighter packing, resulting in a stretching and a reduction of the oleoyl chain cross-section. The nonequivalence of the CD bonds of the α-methylene segment of the lipid choline group observed at $R_{S/L} = 0.2$ (cf. Figure 3b) might be the result of the tight packing of the components at low surfactant concentration.

TABLE 1: Parameters Determined under Equal Conditions (25 °C, Hydration Pressure 4.19 MPa Corresponding to 97% Relative Humidity)

	$R_{S/L}$				
	0 (pure POPC)	∞ (pure $C_{12}E_4$)	0.2	1	absolute error
$I(C_{16})^b$/nm	1.191		1.191	1.140	±0.005[a]
$A(C_{16})^e$/nm^2	0.376		0.376	0.393	±0.001[a]
$I(C_{12})^b$/nm		0.816	0.895	0.867	±0.005[a]
$A(C_{12})^c$/nm		0.446	0.407	0.420	±0.0005[a]
W^d/mol mol^{-1}	13.0	7.5	9.5	19.0	±0.5

[a] The error was calculated according to the assumption of an absolute error for the quadrupolar splitting $\Delta\nu = \pm 0.5$ kHz and the resulting $= \Delta S^i_{mol} = \pm 0.01$. [b] $I(C_{16})$ and $I(C_{12})$: length of the lipid palmitoyl and the surfactant dodecyl chains, respectively. [c] $A(C_{16})$ and $A(C_{12})$: cross-sectional areas of the corresponding chains. [d] W: water molecules sorbed per amphiphilic molecules.

With increasing surfactant concentration, the mismatch of the lipid and surfactant hydrocarbon chain lengths become increasingly a factor of importance. As a consequence, at $R_{S/L} = 1$ the ordering of the lipid palmitoyl chain decreases and hence its length compared with the pure lipid membrane decreases (cf. Figure 1 and Table1). The ordering of the surfactant dodecyl chain decreases, too, compared with that at low surfactant concentration ($R_{S/L} = 0.2$), but it remains still higher compared with the pure surfactant membrane (cf. Figure 2 and Table 1). The main reason is the enlarged repulsion between the ethylene oxide headgroups due to the reduced mean distances between them at higher surfactant concentration. A certain contribution

comes also from the interaction with the lipid acyl chains, the ordering of which decreased with increased surfactant concentration.

The overall effect of the interactions between the surfactant and lipid molecules in the mixtures is the approach of the orderings of the dodecyl and palmitoyl (Figure 6a) and probably also of the oleoyl chains as concluded above. At low surfactant concentration ($R_{S/L} = 0.2$) the approach results almost only from the increase of the ordering of the dodecyl chains due to the decrease of the ethylene oxide repulsion whereas at high surfactant concentration ($R_{S/L} = 1$) the ordering also of the palmitoyl chain changes. This is mainly caused by the mismatch of the lipid and surfactant hydrocarbon chain lengths.

However, the segmental order parameters are very differently influenced by the interactions of the components, as the difference order parameter profiles $\Delta S^i_{mol} = S^i_{mol}$(pure membrane) $- S^i_{mol}$(mixed membrane) for the lipid and surfactant in Figure 6b reveal. The $|\Delta S^i_{mol}|$ of $C_{12}E_4$ and POPC drop for the same segment index ($i = 7$) due to the interaction of the seventh methylene segments of the surfactant dodecyl and lipid palmitoyl chains with the C—C═C—C fragment of the oleoyl chain. The coincidence of the drops evidences that these methylene segments possess on average the same penetration depth in the hydrophobic core. This result fits with the finding that the α-methylene segment of the surfactant dodecyl chain is anchored at the hydrophobic/hydrophilic boundary of the mixed membrane.[12] Obviously, the constraints caused by the mismatch are not reduced by the inclusion of ethylene oxide units into the hydrophobic core but by a fluidization of the palmitoyl (see below) and probably of the oleoyl chains. In other words, the fluidization of the lipid acyl chains is thermodynamically more favorable than the inclusion of the ethylene oxide units into the hydrophobic core.

If we leave the effects of the C—C═C—C fragment out of consideration, we can conclude from Figure 6b that the order parameters of all hydrocarbon segments of the surfactant dodecyl chain are influenced by the surfactant lipid interaction to about the same extent with a slight decrease along the chain approaching the terminal methyl segment whereas those of the lipid palmitoyl chain exhibit varying changes. The order parameters of the first methylene segments ($i \leqslant 5$) of the lipid palmitoyl chain undergo about the same changes. But they are smaller compared with those of the surfactant; that means $|\Delta S^i_{mol}(POPC)| < |\Delta S^i_{mol}(C_{12}E_4)|$ for $i \leqslant 5$ (cf. Figure 6b), which is due to the strong interactions between the upper parts of the acyl chains in the lipid molecule. The order parameters of most of the methylene segments with $6 \leqslant i \leqslant 12$ (middle part of the palmitoyl chain) change more strongly than those of the surfactant; that means $|\Delta S^i_{mol}(POPC)| \geqslant |\Delta S^i_{mol}(C_{12}E_4)|$ for $6 \leqslant i \leqslant 12$ (Figure 6b). The increase of the order parameter decrease ΔS^i_{mol}(POPC) along the chain corresponds to the picture of the effect of the chain mismatch. It is only a very crude one according to Figure 6b, and it fails completely in the case of the end segments of the palmitoyl chain ($i > 12$), for which ΔS^i_{mol}(POPC) decreases rapidly, approaching the terminal methyl segment. Obviously, the disorder of the last segments of the palmitoyl and probably of the oleoyl chains in the pure membrane is already high, so that the incorporation of surfactant increases more the disorder of the others, especially the chain segments of the middle part of the palmitoyl chain. It should be stressed that this concerns the three segments by which the palmitoyl chain is longer than the dodecyl chain. This fact gives the indication that the terminal methyl segment of the surfactant dodecyl chain penetrates the hydrophobic core to the same depth as the first twelve methylene segments of the lipid palmitoyl chain.

Mixed Membranes, Headgroups. The lipid surfactant interactions simultaneously modify the headgroup characteristics (Figures 3 and 4). The changes of the methylene quadrupole splittings of the lipid choline group (decrease of the α- and increase of the β-splittings; Figure 3) correspond to a reorientation of the phosphorus nitrogen connecting vector in the direction of the membrane director.[33] The Monte Carlo simulations (cf. Figure 5) suggest that the lipid headgroup reorientation can be explained by the weakening of the electrostatic dipole−dipole interactions between the headgroups. Previous simulations showed that the headgroups tend to lie in the plane due to electrostatic interaction. Shielding of this interaction had the same effect as a dilution of the lipid: The lateral ordering decreases on one hand, as visible in the snapshots; on the other hand, the headgroups tilted upward. The dilution of the lipid is equivalent to the incorporation of surfactant molecules into the lipid matrix in the framework of the model and leads to the same effects as observed experimentally.

Simultaneously with the lipid headgroup reorientation, the conformations of the surfactant headgroup drastically change. The incorporation of surfactant into the lipid ($R_{S/L} = 0.2$) decreases the quadrupole splitting of all methylene segments of the ethylene oxide chain except the first α-segment (Figure 4), indicating more motional freedom. If the ethylene oxide chains in the pure surfactant membrane possess effective structures of relatively short rods, the axes of which are on average oriented in parallel to the membrane director, they adopt more laterally extended structures in the lipid matrix ($R_{S/L} = 0.2$), which one can imagine as pearlike structures anchored at the hydrophobic hydrophilic interface. At $R_{S/L} = 1$ the NMR splitting pattern looks again more like that of the pure surfactant L_α phase (cf. Figure 4b), indicating that the pearlike structure transforms into the conformation present in the pure surfactant membrane, increasing the surfactant concentration.

The different structural characteristics are correlated to considerable modifications of the hydration properties of the membranes as the various amounts of water sorbed under the same conditions indicate (see paragraph 2, Substances and Sample Preparation). They correlate also with dynamic processes in the mixed membranes.[39]

5. Conclusions

The thickening of the bilayer and its hydrophobic core incorporating small amounts of surfactant ($R_{S/L} = 0.2$) into the lipid matrix, which was found in ref 11, is mainly the result of the stretching of the surfactant dodecyl chain which is primarily caused by the reduction of the surfactant headgroup repulsions. The lipid molecules act as lateral spacers and, as a consequence, the surfactant ethylene oxide chains adopt a pearlike effective structure. Compared with the pure surfactant membrane,[11] this structure has a bigger accessibility for water in agreement with the higher differential water uptake. The lateral extension and the higher water uptakes lead to a bigger surface requirement of the surfactant in the lipid matrix which was found in ref 11.

Simultaneously, the tighter packing mainly of the lipid oleoyl chains induced by the surfactant gives a smaller lipid surface requirement, which was also found by König.[11] Further, the reduction of the surface requirement decreases the lipid hydration and the water uptake measured (9.5 water per amphiphilic molecule; $R_{S/L} = 0.2$).

With increasing surfactant concentration, the mismatch of the lipid and surfactant hydrocarbon chain lengths become a factor

of increasing importance. At $R_{S/L} = 1$ it leads to an increase of the disorder mainly of the middle part (sixth to the twelfth methylene segments) of the lipid palmitoyl and probably also of the oleoyl chains. Since the first seven methylene segments of the surfactant dodecyl and lipid palmitoyl chains penetrate the hydrophobic core to the same depth on average, we conclude that the increase of the lipid acyl chain disorder is thermodynamically more suitable to cope for the mismatch than the inclusion of ethylene oxide units into the hydrophobic core. Simultaneously, the mean orientation of the lipid headgroup changes. It shifts progressively in the direction of the membrane director with increasing surfactant concentration due to the weakening of the electric dipole−dipole interactions between the lipid headgroups.

The fluidization of the lipid acyl chains causes an increase of the lipid surface requirement. Together with the lipid headgroup reorientation, which increases the accessibility for water and fits better the net of water structures around the headgroup, it leads to the relatively high water uptake by the mixed membrane (19.0 water per amphiphilic molecules at $R_{S/L} = 1$). The pearlike structure of the surfactant ethylene oxide chains transforms to that of the pure surfactant membrane (short rods with axes in parallel to the membrane director), increasing the surfactant concentration.

Acknowledgment. The authors thank Mrs. Dietrich for measuring the water sorption of the samples and Prof. Levine (University Utrecht) for helpful discussion. We gratefully acknowledge the financial support of the Deutsche Forschungsgemeinschaft (SFB 294, C7) and the Bundesministerium für Bildung, Wissenschaft, Forschung, und Technologie BMBF (03-DUBLEI-5).

References and Notes

(1) Heerklotz, H.; Binder, H.; Lantzsch, G.; Klose, G. *J. Phys. Chem. B* **1997**, *101*, 639.
(2) Moller, J. V.; Le Maire, M.; Andersen, J. P. *Progress in Protein−Lipid-Interactions*; Elsevier: Amsterdam, 1986; Vol. 1.
(3) Levy, D.; Gulik, A.; Seigneuret, M.; Rigaud, J. L. *Biochemistry* **1990**, *29*, 9480.
(4) Paternostre, M. T.; Roux, M.; Rigaud, J. L. *Biochemistry* **1988**, *27*, 2668.
(5) Krämer, R. *Biochim. Biophys. Acta* **1994**, *1185*, 1.
(6) Klose, G.; Eisenblätter, S.; König, B. *J. Colloid Interface Sci.* **1995**, *172*, 438.
(7) Funari, S. S.; Klose, G. *Chem. Phys. Lipids* **1995**, *75*, 145.
(8) Mädler, B.; Binder, H.; Klose, G. *J. Colloid Interface Sci.* **1998**, *202*, 124.
(9) Lantzsch, G.; Binder, H.; Heerklotz, H.; M., W.; Klose, G. *Biophys. Chem.* **1996**, *58*, 289.
(10) Arnold, K.; Lvov, Y. M.; Szögyi, M.; Györgyi, S. *Stud. Biophys.* **1986**, *113*, 7.
(11) König, B.; Dietrich, U.; Klose, G. *Langmuir* **1997**, *13*, 525.
(12) Klose, G.; Islamov, A.; Koenig, B.; Cherezov, V. *Langmuir* **1996**, *12*, 409.
(13) Struppe, J.; Noack, F.; Klose, G. *Z. Naturforsch.* **1997**, *52A*, 681.
(14) Israelachvili, J. N.; Marcelja, S.; Horn, R. G. *Q. Rev. Biophys.* **1980**, *13*, 121.
(15) Davis, J. H. *Biochim. Biophys. Acta* **1983**, *737*, 117.
(16) Bloom, M.; Evans, E.; Mouritsen, O. G. *Q. Rev. Biophys.* **1991**, *24*, 293.
(17) Mouritsen, O. G.; Bloom, M. *Annu. Rev. Biophys. Biomol. Struct.* **1993**, *22*, 145.
(18) Morrison, C.; Bloom, M. *J. Chem. Phys.* **1994**, *101*, 749.
(19) Binder, H.; Anikin, A.; Kohlstrunk, B.; Klose, G. *J. Phys. Chem. B* **1997**, *101*, 6618.
(20) Seelig, J. *Q. Rev. Biophys.* **1977**, *10*, 353.
(21) Groetsch, C. W. *The Theory of Tikhonov Regularization for Fredholm Integral equations of the First Kind*; Pitman: London, 1984.
(22) Schäfer, H.; Mädler, B.; Volke, F. *J. Magn. Reson. A* **1995**, *116*, 145−149.
(23) Schäfer, H.; Mädler, B.; Sternin, E. *Biophys. J.* **1998**, *74*, 1007.
(24) Glaubitz, C.; Schäfer, H.; Mädler, B.; Klose, G.; Watts, A. Manuscript in preparation.
(25) Schindler, H.; Seelig, J. *Biochemistry* **1975**, *14*, 2283.
(26) Salmon, A.; Dodd, S. W.; Williams, G. D.; Beach, J. M.; Brown, M. F. *J. Am. Chem. Soc.* **1987**, *109*, 2600.
(27) Seelig, A.; Seelig, J. *Biochemistry* **1974**, *13*, 4839.
(28) Nagle, J. F.; Wilkinson, D. A. *Biophys. J.* **1978**, *19*, 159.
(29) Schneider, K. P.; Keller, J. *Chem. Phys. Lett.* **1997**, *275*, 63.
(30) Seelig, J.; Waespe-Sarcevic, N. *Biochemistry* **1978**, *17*, 3310.
(31) Gawrisch, K.; Ruston, D.; Zimmerberg, J.; Paesegian, A.; Rand, P.; Fuller, N. *Biophys. J.* **1992**, *61*, 1213.
(32) Tocanne, J. F. *Biochim. Biophys. Acta* **1990**, *1031*, 111.
(33) Seelig, J.; MacDonald, P. M.; Scherer, P. G. *Biochemistry* **1987**, *26*, 7535.
(34) Frischleder, H.; Peinel, G. *Chem. Phys. Lipids* **1982**, *30*, 121.
(35) Heller, H.; Schaefer, M.; Schulten, K. *J. Phys. Chem.* **1993**, *97*, 8343.
(36) Fattal, D. R.; Ben-Shaul, A. *Biophys. J* **1994**, *67*, 983.
(37) Ward, A. J. I. *Mol. Cryst. Liq. Cryst.* **1988**, *154*, 55.
(38) Mädler, B.; Klose, G.; Möps, A.; Richter, W.; Tschierske, C. *Chem. Phys. Lipids* **1994**, *71*, 1.
(39) Kukla, V.; Kärger, J.; Klose, G. *J. Phys. Chem.*, submitted.